Available online at www.sciencedirect.com
SCIENCE DIRECT®
PERGAMON
International Journal of Heat and Mass Transfer 46 (2003) 3673–3682
International Journal of HEAT and MASS TRANSFER
www.elsevier.com/locate/ijhmt

Subcooled flow boiling heat transfer in narrow passages

B.S. Haynes *, D.F. Fletcher [1]

Department of Chemical Engineering, University of Sydney, Sydney, NSW 2006, Australia

Received 30 June 2002; received in revised form 7 March 2003

Abstract

Subcooled flow boiling heat transfer coefficients for refrigerants R11 and HCFC123 in smooth copper tubes of small diameter have been investigated experimentally. The parameter ranges examined are: tube diameters of 0.92 and 1.95 mm; heat fluxes 11–170 kW m^{-2}; mass fluxes 110–1840 kg m^{-2} s^{-1}. The range of liquid Reynolds numbers encompassed by the data set is 450 to 12,000.

The data in the subcooled and saturated regions are well represented by the simple addition of convective and nucleate boiling heat transfer contributions

$$h = h_{\mathrm{conv}} + h_{\mathrm{pb}}(q_{\mathrm{nb}})\frac{\Delta T_{\mathrm{sat}}}{\Delta T_{\mathrm{mean}}}$$

where the nucleate component is found to be represented best by the Gorenflo pool boiling correlation using $q_{\mathrm{nb}} = q_{\mathrm{tot}} - q_{\mathrm{conv}}$. The convective component is calculated as for single-phase liquid-only heat transfer, with due allowance for laminar entrance effects. There is no evidence that convection suppresses the nucleate term nor that nucleation events enhance the convective term, even in laminar and transitional flows. However, the laminar flows, in particular, are prone to enhancement by unknown mechanism, possibly by outgassing of the fluid as it is heated through the subcooled region.

Keywords: R11; HCFC123; Narrow passage; Microchannel; Subcooled flow boiling; Saturated flow boiling; Nucleate boiling

1. Introduction

Subcooled boiling of a liquid can occur when the liquid is exposed to a hot surface, providing the surface temperature is sufficiently above the fluid saturation temperature. The generated vapour may recondense while the bulk fluid enthalpy remains below its saturation value but the formation and behaviour of even transitory bubbles may have a profound impact on the heat transfer between the hot wall and the bulk fluid.

For a fluid flowing in a heated pipe, the subcooled region may be divided into a number of zones, as described by Collier and Thome [1] or by Schröder [2]. The initial formation of bubbles, known as the onset of nucleate boiling, ONB [1], occurs when the wall temperature exceeds the fluid saturation temperature sufficiently to allow bubbles to nucleate. At low heat fluxes, or high extents of subcooling, the rate of generation of bubbles is well below that corresponding to fully developed nucleate boiling and the bubbles do not penetrate to the bulk fluid, either collapsing immediately or being convected along with the flow at the wall. As the fluid approaches saturation, the surface becomes fully active for nucleation and we obtain a net generation of vapour that may begin to penetrate into the bulk fluid. The impact of the incipient bubbles, at the onset of nucleate boiling, on the wall temperature may be quite profound, with the wall temperature decreasing sharply at this point. Under fully developed but still subcooled conditions, the wall temperature takes a

* Corresponding author. Tel.: +61-2-9351-3435; fax: +61-2-9351-3471.
E-mail addresses: haynes@chem.eng.usyd.edu.au (B.S. Haynes), davidf@chem.eng.usyd.edu.au (D.F. Fletcher).
[1] Tel.: +61-2-9351-4147.

0017-9310/03/$ - see front matter
doi:10.1016/S0017-9310(03)00172-8

Nomenclature

A	area (m^2)
d	diameter (m)
G	mass flux ($kg\,m^{-2}\,s^{-1}$)
h	heat transfer coefficient ($kW\,m^{-2}\,K^{-1}$)
k	thermal conductivity ($W\,m^{-1}\,K^{-1}$)
Nu	Nusselt number, hd/k (–)
ONB	onset of nucleate boiling
p	pressure (kPa)
q	wall heat flux ($kW\,m^{-2}$)
Q	heat flow rate (W)
Re	Reynolds number, Gd/μ (–)
x	thermodynamic quality (–)
z	axial distance (m)

Greek symbol

μ	viscosity (Pa s)

Subscripts and superscripts

conv	convective
crit	critical Re at which laminar/turbulent transition occurs
exptl	experimental
LO	liquid-only
nb	nucleate boiling
pb	pool boiling
pred	predicted
sat	saturated

value very close to that corresponding to saturated boiling.

Some very complex approaches have been developed to calculate the heat transfer coefficient in the subcooled region, from ONB, through partial subcooled flow boiling, to fully developed subcooled and saturated nucleate boiling [1,3,4]. Phenomenologically, the issue is to account for both nucleate and convective effects, and their potential interaction. Perhaps the simplest approach for modelling this behaviour is that developed for saturated flow boiling by Chen [5] in which the two contributions operate in parallel, with bulk and saturation temperature driving forces for the convective and nucleate components, respectively. Thus,

$$q = q_{\mathrm{conv}} + q_{\mathrm{nb}} = h_{\mathrm{conv}}(T_{\mathrm{W}} - T_{\mathrm{mean}}) + Sh_{\mathrm{pb}}(T_{\mathrm{W}} - T_{\mathrm{sat}}) \quad (1)$$

where S accounts for the suppression of nucleate boiling by convective effects. While there is in fact some debate over whether there is such a phenomenon as "suppression of nucleate boiling" [1,6], it is reported [5] that, for $Re_{\mathrm{LO}} < 10,000$, $S \to 1$ in any case. Furthermore, our own earlier work on saturated nucleate boiling in fine passages under nominally laminar and transitional flow conditions ($500 < Re_{\mathrm{LO}} < 12,000$) showed no evidence of convective effects [7]. We therefore take $S = 1$ in applying Chen's [5] method to our data.

If the apparent heat transfer coefficient is defined in terms of the bulk mean temperature difference, $h_{\mathrm{app}} = q/(T_{\mathrm{W}} - T_{\mathrm{mean}})$, then:

$$h_{\mathrm{app}} = h_{\mathrm{conv}} + h_{\mathrm{pb}}\frac{(T_{\mathrm{W}} - T_{\mathrm{sat}})}{(T_{\mathrm{W}} - T_{\mathrm{mean}})} = h_{\mathrm{conv}} + h_{\mathrm{pb}}\frac{\Delta T_{\mathrm{sat}}}{\Delta T_{\mathrm{mean}}} \quad (2)$$

The above equation shows very simply that a decrease in h_{app} with increasing subcooling ($\Delta T_{\mathrm{sat}}/\Delta T_{\mathrm{mean}} \to 0$) is to be expected. This is of course not the same as suppression of nucleate boiling by convective effects but it does mean that convection becomes the dominant heat transfer mechanism at high degrees of subcooling, whether or not subcooled nucleate boiling is fully developed.

The question now is to estimate h_{conv} for subcooled conditions. It has been suggested [1] that this should be taken as the single phase (turbulent) liquid heat transfer coefficient without any need to allow for the enhancement of convection by nucleate phenomena. This seems reasonable for turbulent conditions, but it is not at all clear that nucleation and transitory bubble formation could not promote bulk heat transfer beyond what can be achieved via laminar conduction. Indeed, Bergles and Rohsenow [4] found that transitional water flows in fine passages ($d = 1.2$ mm, $Re \sim 4500$) could be tripped into turbulence by incipient boiling, thus promoting the convective heat transfer.

We recently reported that h_{conv} is far larger than its single-phase value in laminar flows, and that this term is strongly correlated with the nucleate boiling term [8]. In this paper, we report on results obtained for the subcooled boiling behaviour of Freon R11 and HCFC123 in tubes with diameters of ~1 and ~2 mm, over a range of pressure, heat flux, and flow rate. While the results are not definitive mechanistically, they do provide a predictive basis for estimating heat transfer rates in laminar and transitional subcooled flow boiling in narrow passages.

2. Experimental apparatus and procedure

The experiments were performed using the same experimental setup as reported for our saturated boiling data and full details can be found in Bao et al. [7,9]. The key feature of this experimental setup is that it allows the measurement of pseudo-local heat transfer rates. In

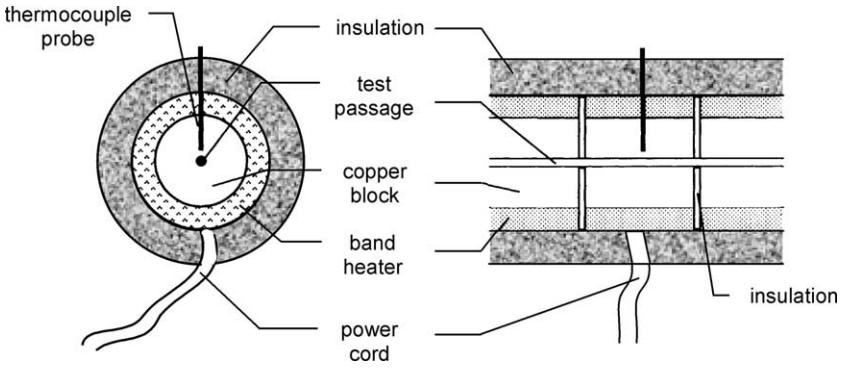

Fig. 1. Schematic of the ohmic heating blocks used to control the heat flux into the fluid.

summary, the experimental apparatus consists of a flow loop, pump and reservoir system. The pressure in the system is controlled by controlling the temperature of the reservoir. The local heat flux to the fluid is controlled by attaching resistance band heaters to each of ten 25 mm diameter copper blocks, each block being 25 mm in length. These blocks are individually soldered to the copper tube that passes longitudinally through their centre, as shown in Fig. 1. Each block is isolated from the next by a 2 mm thickness of compressed fibre insulation. The entire section is wrapped in closed cell foam insulation to minimize ambient heat losses and the effect of environmental changes.

The band heaters are connected in parallel to a variable AC power source and the heat input into each block is calculated from the input voltage and resistance of each band heater. Voltage and resistance are measured with a digital multimeter. The heater resistance was found to be independent of temperature over the range of temperatures experienced during normal operation. The heat losses from the system were measured for the situation with no fluid flow, when there is no heat transfer to the central flow tube at steady state. These data are used to calibrate the heat losses.

When test fluid flows through the system, the input power and measured temperatures can be used to determine the heat losses (which are always less than 5% of the heat input) and the heat flow to the fluid for each block, Q_i, as described in Bao et al. [7,9]. Since the subcooled fluid enthalpy at the inlet to the test section ($\widehat{H}_0$) is known from the inlet temperature, the mean enthalpy at the centre of each block can be calculated from the sum of the heat transfer rates up to that point:

$$\dot{m}(\widehat{H}_i - \widehat{H}_0) = \sum_{j=1}^{i-1} Q_j + \frac{Q_i}{2} \tag{3}$$

The local pressure within the system is estimated from the overall measured pressure drop using the Lockhart–Martinelli [1] procedure to interpolate between the measured inlet and outlet pressures [10,11]. The equilibrium mean fluid properties (for the local pressure and enthalpy) are then obtained from the NIST Refprop 6.01 [12] package. In particular, the thermodynamic quality is calculated as

$$x_{\text{th}}|_i = \left.\frac{\widehat{H} - \widehat{H}_{\text{sat,L}}}{\widehat{H}_{\text{sat,V}} - \widehat{H}_{\text{sat,L}}}\right|_i \tag{4}$$

The experimental overall heat balance for single-phase systems closes within 10% [9]. The relative uncertainty in the change in the fluid enthalpy across the 10-block test section is therefore also of this order, or nominally 1% cumulatively per block. The uncertainty in x_{th} at a particular measurement point can therefore be characterised as

$$\delta x_{\text{th}}|_i \sim \frac{i}{100}(x_{\text{th}}|_{10} - x_{\text{th}}|_0) \tag{5}$$

Note that the overall Δx_{th} varies as the ratio of wall heat flux to fluid mass flux. For the present results in the subcooled and early saturated boiling regions ($-0.2 < x_{\text{th}} < 0.2$), the uncertainty in the local value of x_{th} is always less than 0.04, and generally below 0.02.

The local heat transfer coefficient is obtained from

$$h_i = \left.\frac{(Q/A)}{T_{\text{W}} - T_{\text{mean}}}\right|_i \tag{6}$$

Estimates of the uncertainties in the individual measurements needed to evaluate h are presented in Table 1. Measurements of local single-phase heat-transfer coefficients in thermally-developing laminar flow agree with theoretical predictions within 10%; the same levels of agreement with correlations for transitional and turbulent flow are also obtained [7]. The only additional source of error in the boiling experiments is in the estimation of T_{sat} which is calculated from the estimate of the local pressure, but this is a minor effect because of the relatively small pressure drops across the test sections [7]. The resulting uncertainty in the boiling heat

Table 1
The range of experimental parameters studied for flow boiling heat transfer. These ranges cover both the saturated and subcooled data

Parameter	Range	Uncertainty
Fluid	HCFC123, R11	
Passage diameter, d	0.92, 1.95 mm	±1%
System pressure, p	215–510 kPa	±0.2% at entry
Mass flux, G	110–1840 $kg\,m^{-2}\,s^{-1}$	±5%
Heat flux, q	11–170 $kW\,m^{-2}$	±5%
Thermodynamic vapour quality, x_{th}	−0.35 to 1.0	±0.04 (see text)
Liquid Reynolds number, Re_{LO}	450–12,000	
Heat transfer coefficient, h	0.5–20 $kW\,m^{-2}\,K^{-1}$	15%

transfer coefficients is therefore no more than 15% of the measured value.

Before new test fluids were loaded into the system, the system was evacuated to <10 Pa. The fluid was then drawn as a liquid into the system and circulated by the pump. The boiling section and the pressure-control reservoir was heated and the system pressurised. In order to outgas the system, the head space above the liquid in the heated pressure-control reservoir was repeatedly flashed to vent, as was the circulating fluid.

The experimental conditions covered in this study are given in Table 1. These correspond with those used in the saturated boiling work reported previously [7,8].

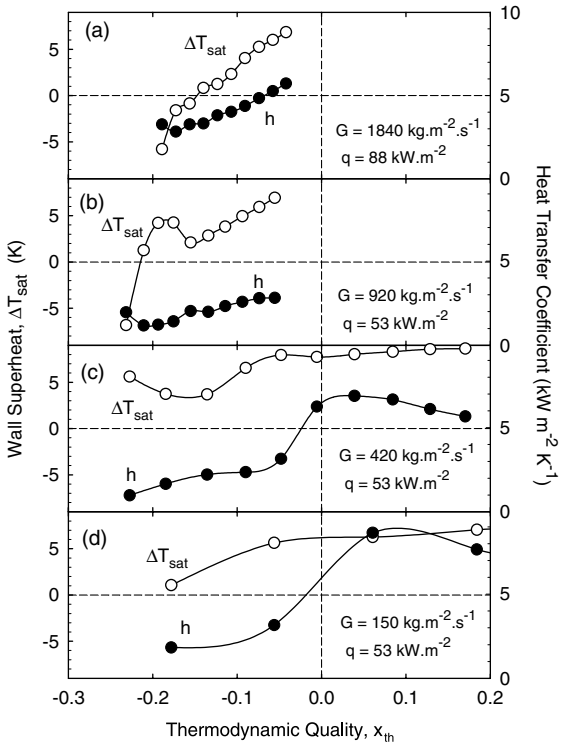

Fig. 2. Variation of wall superheat (ΔT_{sat}) and bulk-mean heat transfer coefficient (a) in subcooled and early saturation conditions for a range of mass fluxes of R11. The heat flux is 88 $kW\,m^{-2}$ in (a) and 53 $kW\,m^{-2}$ in (b)–(d). The liquid Reynolds numbers in the flows entering the heated section are (a) 9300, (b) 4700 (c) 2200, and (d) 850.

3. Results

Fig. 2 shows results for wall superheat (ΔT_{sat}) and apparent heat transfer coefficient ($h = q/\Delta T_{mean}$) for four runs over a wide range of mass flux. The test fluid is R11 flowing in a 1.95 mm diameter tube. The system pressure is 350 kPa ($T_{sat} = 64.1$ °C) for the data in Fig. 2(a), and 435 kPa ($T_{sat} = 72.5$ °C) for Fig. 2(b)–(d). The range of liquid Reynolds number in the subcooled entry region is from 9300 in Fig. 2(a) to 850 in Fig. 2(d).

In each panel, the data point at the lowest value of x_{th} corresponds to the first block in the section, with subsequent blocks in ascending order of x_{th}. For higher values of q/G in panel (d), the results extend well into the saturated boiling regime ($x_{th} > 0.2$). Our data in this region have been presented previously in detail [7–11] and are not reproduced here.

Classical ONB behaviour is most easily identified in Fig. 2(b), in which the wall superheat shows a distinct maximum after which the heat transfer coefficient begins to rise as the fluid approaches saturation. When the fluid velocity is decreased, the ONB occurs earlier in the test section and the maximum in the wall superheat is not discernible. In Fig. 2(c), we can still see the decrease in wall superheat as the heat transfer coefficient begins to rise, but at the lowest velocities, as in Fig. 2(d), even this feature is submerged inside the first test block.

The results at the highest velocity, in Fig. 2(a) do not show any overshoot in the wall superheat. In this case, the high liquid velocity is accompanied by a high liquid heat transfer coefficient (apparent in the region where boiling cannot possibly occur, $\Delta T_{sat} < 0$). When boiling is initiated, the enhancement of the heat transfer coefficient beyond its liquid-only value is relatively weak and there is no apparent reduction in the wall superheat.

The full data set consists of more than 2000 points obtained over the range of conditions specified in Table 1.

4. Discussion

The implication of the above result is that there are effects of mass flux on the heat transfer coefficients in the

subcooled region, but they are not easily identified at lower flow rates. Thus, for example, at $x_{th} = -0.1$ in Fig. 2(b)–(d), h takes a value of 2.2 ± 0.2 kW m^{-2} K^{-1}, independent of mass flux, even though the convection-only heat transfer coefficient is expected to vary by a factor of 5 between these runs. The analysis of the observations is complicated by the occurrence of different flow regimes (laminar and transitional) and by entry effects.

For transitional turbulent flows ($2300 < Re < 10,000$), the Petukhov–Gnielinski correlation [13] may be used to estimate the single-phase convection heat transfer coefficient:

$$Nu = \frac{(Re - 1000)Pr\frac{f}{2}}{1.07 + 12.7(Pr^{2/3} - 1)\sqrt{\frac{f}{2}}}, \quad \text{where}$$
$$\frac{f}{2} = 0.0396Re^{-0.25} \tag{7}$$

Thermal entry effects in turbulent flows with $Pr \sim 3$ are negligible [14] but this is not the case for the laminar flows. In the experiments, the flows are fully developed hydrodynamically by passage through a 400 mm ($L/d > 200$) unheated entry zone. However, the first measurement location within the heated section (Block 1) occurs 12.5 mm ($L/d \sim 6$) downstream, with subsequent measurements every 27 mm. Taking the thermal entry length as $L_{th}/d \sim 0.04RePr$ [15], we see that entry effects arise for >100 diameters downstream, potentially encompassing most of the blocks in the test section.

The individual copper blocks defining each heating zone in the experiments are very nearly isothermal, but, in going from one block to the next while the fluid is undergoing purely sensible heating, there is a step change in the wall temperature [9]. On the other hand, each block is constrained to having very nearly the same average heat flux. The experiments therefore do not correspond precisely to any of the standard thermal boundary conditions for which analytical laminar-flow solutions are available [15]. This has been investigated experimentally for single phase flows [10,11] and the results have been found to be in excellent quantitative agreement with the theoretical expectations [15] for the local Nusselt number at constant heat flux, $Nu_{z,H}$, based on the total length from the start of the test section. This is about 25% higher than the predicted local Nusselt number for the constant wall temperature condition, $Nu_{z,T}$, possibly because of the thermal perturbation of the boundary layer at each new block. We therefore assume that laminar-flow convective heat transfer coefficients for the present work may be estimated from the following fit (accurate to within 7%) to the analytical result for $Nu_{z,H}$:

$$Nu_{z,H} = 4.364 + \frac{0.0273}{z^* + 0.0236(z^*)^{1/3}},$$
$$z^* \geqslant 10^{-5}, \qquad \text{where } z^* = \frac{z/d}{RePr} \tag{8}$$

For transitional flows, we use the greater of the developing laminar heat transfer coefficient (Eq. (8)) and the Gnielinski value (Eq. (7)), on the assumption that the local heat transfer coefficient cannot be lower than is estimated for the laminar condition. This is only an issue when Re is near the transitional value (Re_{crit} is assumed to be 2300), and then only in the first one or two blocks.

4.1. Saturated boiling

In order to examine the applicability of Eq. (1) to subcooled boiling, we have first confirmed its suitability to saturated boiling, under which conditions $\Delta T_{mean} = \Delta T_{sat}$. We estimate the experimental nucleate boiling heat transfer coefficient from the additive model,

$$h_{nb}^{exptl} = h - h_{conv} \tag{9}$$

and we compare that value with that predicted for the prevailing nucleate boiling flux using the Gorenflo correlation [16]:

$$h_{pb} = f_{Gorenflo}(q_{nb}), \quad \text{where } q_{nb} = q - q_{conv}$$
$$= q - h_{conv}\Delta T_{mean} \tag{10}$$

In applying the Gorenflo method, a reference nucleate boiling heat transfer coefficient of $h_0 = 2.8$ kW m^{-2} K^{-1} has been assumed for R11; for HCFC123, $h_0 = 2.6$ kW m^{-2} K^{-1}. The tube surface roughness was taken as 1 μm.

Figs. 3 and 4 show that the agreement between the predictions and the measured values are very good across the whole data set, which consists of 442 points for R11 (all with $d = 1.95$ mm) and HCFC123 (Fig. 4, 130 points with $d = 1.95$ mm, and 261 points with $d = 0.92$ mm). For both fluids, the average relative error $|h_{pred} - h_{exptl}|/h_{exptl} < 10\%$. There is little scatter in the relative error in the larger tube (relative standard deviation <10% for R11 and <5% for HCFC123) but there is more scatter with the smaller pipe (HCFC123 only, relative standard deviation 20%). Given the estimated 15% uncertainty in the experimental values, the agreement between the experimental data and the predictions shown in Figs. 3 and 4 is extremely good. Many of the cases have $Re_{LO} < Re_{crit}$ and are predicted to have relatively small single-phase convective heat transfer coefficients, accounting for 3–10% of the measured value, for more than 90% of our data points. From the results of Bergles and Rohsenow [4], obtained with water in a 1.2 mm passage, it might be expected that bubble formation

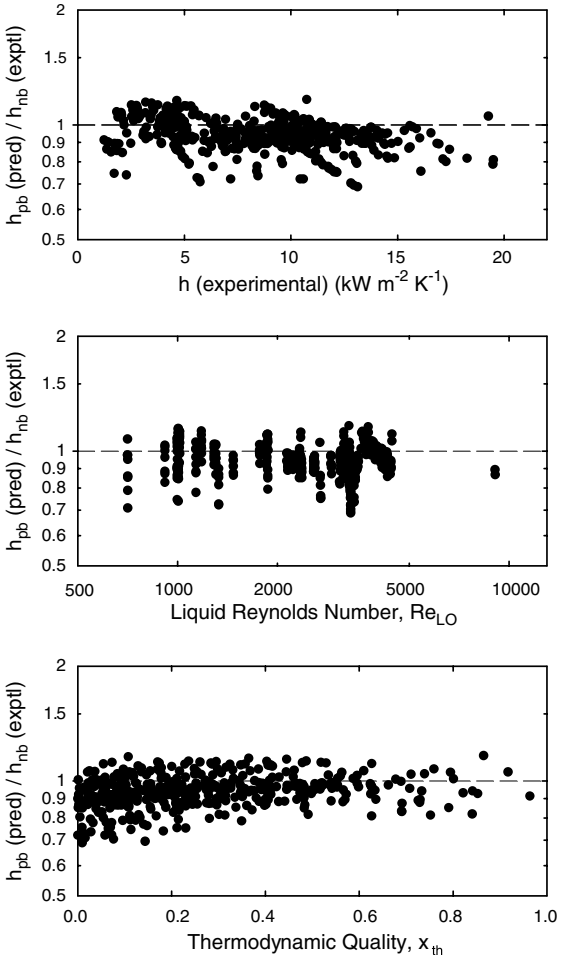

Fig. 3. Summary of comparison of all data for saturated flow boiling of R11 with predictions of the Gorenflo [16] method. The data were obtained in tubes with $d = 1.95$ mm over the range of conditions shown in Table 1.

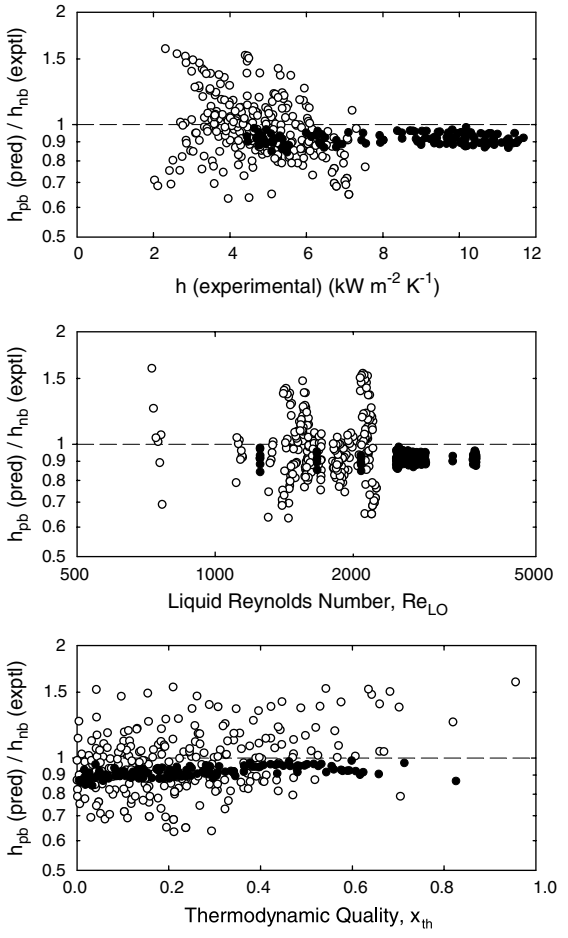

Fig. 4. Summary of comparison of all data for saturated flow boiling of HCFC123 with predictions of the Gorenflo [16] method. The data were obtained in tubes with $d = 1.95$ mm (filled symbols) and $d = 0.92$ mm (open symbols) over the range of conditions shown in Table 1.

would promote bulk turbulence in these flows, especially in those close to the laminar/turbulent transition, thus enhancing the bulk convective contribution to total heat transfer coefficient. However, it is clear from the figures that any such effect must still be small compared with the convective effects already embodied in the nucleate pool boiling heat transfer mechanism. In essence, the contribution of single-phase laminar and transitional forced convection to saturated boiling heat transfer is very weak. This is in agreement with other experimental observations of boiling in microchannels, as summarised recently by Palm [17].

We have previously compared some of our data in the saturated region with other pool boiling correlations [7,8] and found reasonable agreement e.g. with the Cooper correlation [18]. In our previous presentations, we took no account of any possible convective contributions, whereas these are now included and are not always negligible: in our most turbulent runs ($Re_{LO} \sim 8000$), the predicted convective contribution may reach 25% of the observed heat transfer coefficient. Overall, however, if we apply the Gorenflo method to all the data, neglecting convective effects, the average ratio of prediction to experiment rises by about 10%, with only a slight (not statistically significant) rise in standard deviation. Therefore, the general improvement in the correlation between measurement and prediction cannot be ascribed to the inclusion of convective effects and reflects the intrinsic accuracy of the Gorenflo method. This method is clearly superior also in providing equally good predictions over the whole range of conditions tested, as shown in Figs. 3 and 4.

4.2. Convective contributions around ONB

Fig. 5 shows the results of applying Eq. (2) to the subcooled and early saturation regions when the Gorenflo method is used to estimate h_{pb} and the convective heat transfer contribution is estimated as described above. The data are for the runs presented in Fig. 2 which reveals that the first few points in Fig. 5(a) and (b) occur in a region where $\Delta T_{sat} < 0$ and correspond to single phase flow. In these turbulent cases there is evidence of an entrance effect in that the first block reports higher values of h than the following blocks, the relative effect being greater at $Re = 4700$ (b) than at $Re = 9300$ (a). This effect is not allowed for in the method for predicting h_{conv} but the fully developed values agree well with the predictions. Once $\Delta T_{sat} > 0$ and nucleate boiling commences, the predictions based on Eq. (2) are in every case, (a)–(d), well represented by the prediction method. In Fig. 5(a), the convective component contributes at least 50% of the total heat transfer coefficient throughout the measurement range, but this fraction falls steadily as the fluid velocity diminishes, 5(b)–(d). At the lowest flows, the convective component is essentially negligible except prior to ONB and under highly subcooled conditions.

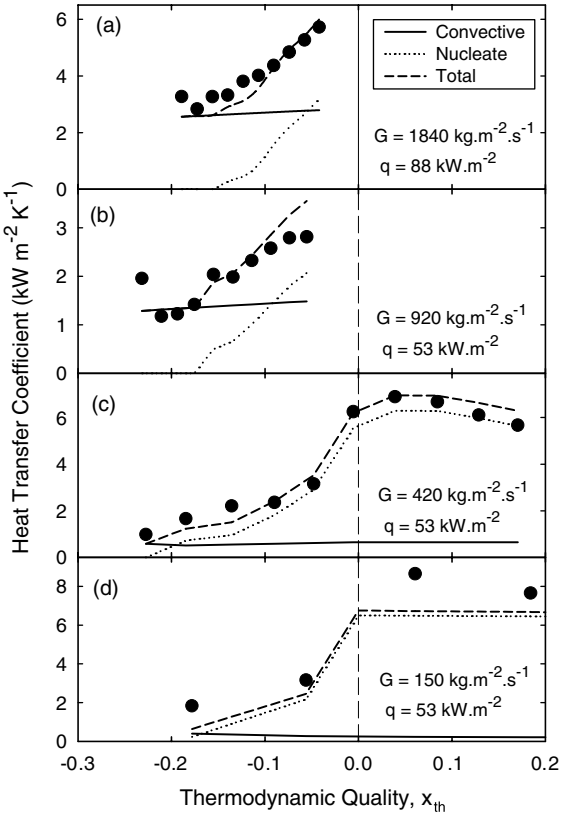

Fig. 5. Comparison of experimental and predicted evolution of the heat transfer coefficient through the subcooled and early saturation conditions for the runs shown in Fig. 2. The prediction is based on the simple addition of pure convective and scaled nucleate components as described by Eq. (2).

4.3. Correlation of subcooled data

Figs. 6 and 7 summarise the agreement between prediction and measurement for all the subcooled data for R11 (324 points, all with $d = 1.95$ mm) and HCFC123 (100 points with $d = 1.95$ mm, and 166 points with $d = 0.92$ mm), respectively. The fraction of the total heat transfer coefficient arising from convective effects in these subcooled data is predicted to be in the range 3–100%. Considering the R11 data, we see that, when the prediction is dominated by the nucleate component (large values of h, or $x_{th} > -0.1$), the agreement

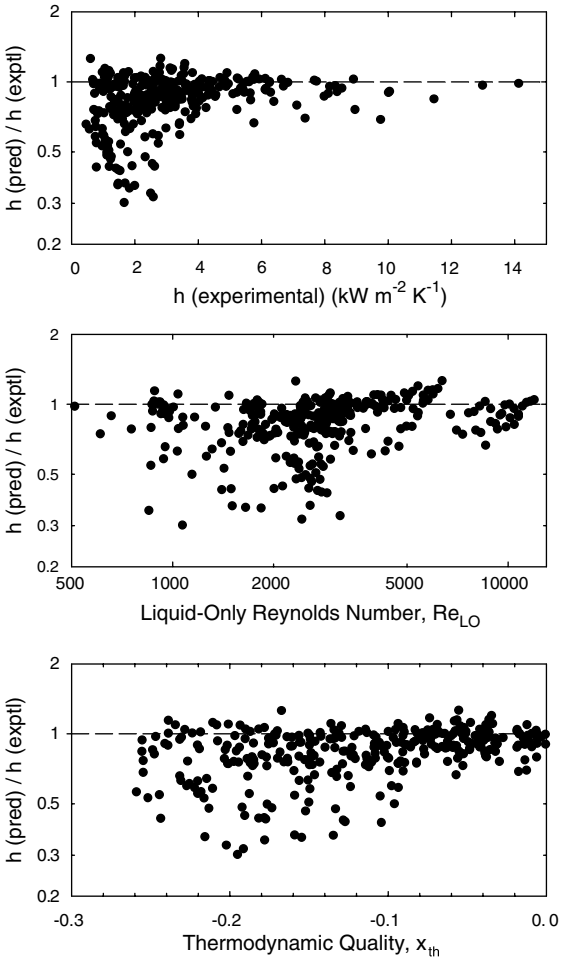

Fig. 6. Summary of comparison of all R11 data in the subcooled region with predictions of the additive flux model, Eq. (2). The data were obtained in tubes with $d = 1.95$ mm over the range of conditions shown in Table 1.

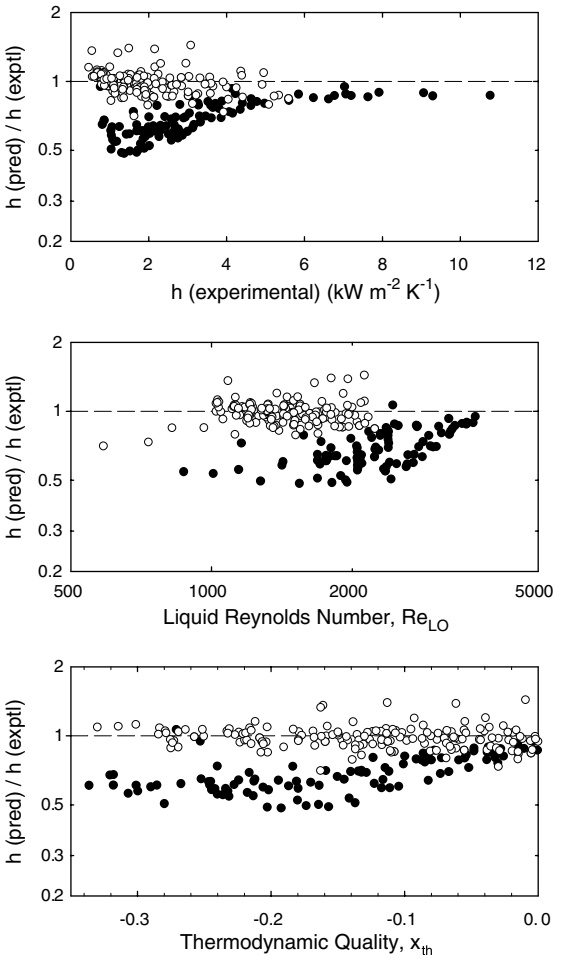

Fig. 7. Summary of comparison of all HCFC123 data in the subcooled region with predictions of the additive flux model, Eq. (2). The data were obtained in tubes with $d = 1.95$ mm (filled symbols) and $d = 0.92$ mm (open symbols) over the range of conditions shown in Table 1.

between experiment and prediction is generally good. However, a significant number (~60) of the data points have $h_{\text{pred}}/h_{\text{exptl}} < 0.7$, indicating significant underprediction of the experimental results. The point at $x_{\text{th}} = -0.18$ in Fig. 5(d) is one of the worst examples of such a point ($h_{\text{pred}}/h_{\text{exptl}} = 0.35$)—on an absolute scale the error is small, even compared with deviations at other blocks in the same run, but the significance of the error in a description of the phenomena at the location in question remains significant. The effect is also present in Fig. 5(c) but is barely discernible at all there.

Similar, although more systematic, trends are observed in the HCFC123 data from the 1.95 mm tube, but the data from the 0.95 mm tube do not exhibit this behaviour. Indeed, the scatter in the comparison between prediction and experiment in the 0.92 mm tube (relative standard deviation = 11%) is significantly less than that for the same data set in the saturation region (Fig. 4, relative standard deviation = 20%), indicating that the inclusion of convective effects (which now contribute between 5% and 100% of the total heat transfer) has led to an overall improvement in the predictions.

The worst deviations in the data comparisons occur when the nucleate contribution is relatively small or formally zero (prior to ONB), and when the convective component itself is small (e.g., at lower *Re*). These are precisely the conditions under which the single-phase (laminar) heat transfer coefficient might be enhanced, for example, by microconvective effects associated with incipient bubble formation [4,8]. However, there is no evidence of such an intrinsic effect in the 0.92 mm data.

We now propose that dissolved gas release may be responsible for the observation of occasional enhancement in the 1.95 mm passage. Close examination of many of the runs indicates that the enhancement occurs after the inlet and before the ONB. The clearest evidence for this hypothesis comes from a run with rather low mass flux and low heat flux ($G = 460$ kg m^{-2} s^{-1}, $Re_{\text{LO}} = 2400$, $q = 30$ kW m^{-2}, $p = 420$ kPa): these conditions provide a low convective heat transfer coefficient and good resolution of the subcooled region, as shown by the profiles of wall superheat and of experimental and predicted heat transfer coefficients presented in Fig. 8. There is no chance of nucleate boiling until at least the sixth block (when ΔT_{sat} first becomes positive) but the wall superheat shows a weak ONB-like local maximum at the second block. There is a convective entrance effect seen in the decrease in h from the first to the second blocks, as seen also in Fig. 5(c). This is followed by a rise in h from block 2 to block 3 to a new level approximately double the predicted (convection-only) value,

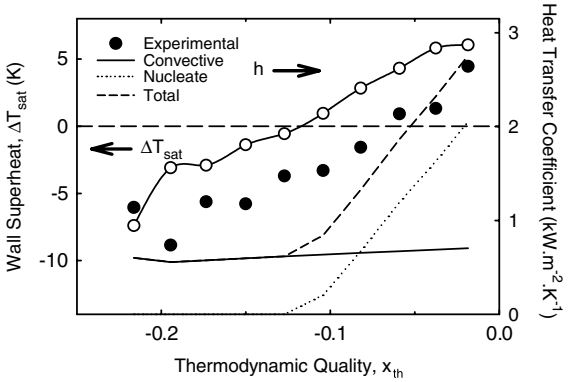

Fig. 8. Wall superheat and measured and predicted heat transfer coefficients for R11 at relatively low heat flux, $q = 30$ kW m^{-2}. The mass flux is $G = 460$ kg m^{-2} s^{-1} ($Re_{\text{LO}} = 2400$), while the tube diameter is $d = 1.95$ mm and pressure is $p = 420$ kPa.

apparently corresponding to the maximum in ΔT_{sat}. After the true ONB at $x_{th} \sim -0.1$, h rises again. Finally, as the saturated region is approached ($x_{th} \to 0$), the measurements and predictions converge as the nucleate component becomes dominant in each. These observations are consistent with the hypothesis that dissolved gas is released as bubbles at some point and that these are responsible for the enhancement of the low values of the liquid-only heat transfer coefficient.

Comparison with our studies of two-phase gas–liquid flows in these passages [9] suggests that a gas mass fraction <0.1% could account for the observed convective enhancement. It is not clear why only the data for the 1.95 mm tube should have been affected but it may be significant that these runs were carried out earlier and with different batches of fluid. In all cases, the procedure for outgassing of the samples was nominally the same, as described in Section 2.

If the explanation for the discrepancy between experiment and prediction in the subcooled region (sporadic for the R11 data, systematic for the HCFC123 data from the 1.95 mm tube) is due to dissolved gas evolution, then the question arises as to what extent the results in the saturated region would be affected by this phenomenon. Clearly, the results where the nucleate term dominates are less likely to be impacted. Moreover, the subcooled HCFC123 results for the $d = 0.92$ mm tube are apparently not affected by gas evolution and have the same mean agreement between experiment and prediction as the affected data. Furthermore, it is only the lowest values of heat transfer coefficient that are significantly enhanced and the absolute magnitude of the enhancement is actually rather small—for example, in Fig. 8, an expected convective heat transfer coefficient of $\sim 0.6\ \mathrm{kW\,m^{-2}\,K^{-1}}$ is measured to be around $1.2\ \mathrm{kW\,m^{-2}\,K^{-1}}$. An effect of this magnitude is essentially negligible in the saturation region and there is no discernible underprediction of h, even at the lowest values of h in Figs. 3 and 4.

Despite the possible occurrence of gas evolution in some of the results, the evidence of Figs. 6 and 7 is that the simple additive mechanism described by Eq. (2) provides an accurate basis for predicting subcooled flow boiling in fine passages. There is no evidence that nucleate boiling phenomena enhance the single-phase convective component, in contrast to our earlier conclusion on this possibility [8]. In many cases, the convective component is negligible once the ONB has occurred, with the result that the effects of mass flux and quality ($x_{th} > 0$) are minimal, as has generally been found in studies of boiling in fine passages. However at very low heat fluxes, or very high mass fluxes, the contribution of (single-phase) convection can be expected to become more significant. This paper has shown that such effects can simply be added to the nucleate boiling component.

5. Conclusions

The low Reynolds numbers that usually pertain to flows in narrow passages lead in general to relatively weak contributions of convective effects in saturated boiling and, once ONB has occurred, in subcooled boiling. We have investigated these in the subcooled flow boiling heat transfer of HCFC123 and R11 in 0.92 and 1.95 mm passages, and conclude that the heat transfer coefficient can be described accurately as a simple additive combination of single-phase liquid-only convection heat transfer and nucleate boiling.

$$h = h_{conv} + h_{pb}(q_{nb})\frac{\Delta T_{sat}}{\Delta T_{mean}}$$

Prior to ONB and under highly subcooled post-ONB conditions ($\Delta T_{sat} \ll \Delta T_{mean}$), the convection component, h_{conv}, is dominant. In many applications, the single-phase liquid-only flow is laminar or transitional and entrance effects may be important in determining the convective component.

The nucleate component becomes more important and ultimately dominates as the subcooled liquid approaches saturation, especially if the heat flux is high or the fluid mass flux is low. This term is accurately represented by the Gorenflo correlation for pool boiling, $h_{Gorenflo}(q_{nb})$, where the nucleate boiling heat flux is estimated as $q_{nb} = q - h_{conv}\Delta T_{mean}$. There is no evidence of suppression of nucleate boiling due to convective effects, which is consistent with the belief either that this phenomenon does not exist at all, or that any such effect would be negligible at low Reynolds numbers.

Once the ONB is reached, the addition of the nucleate mechanism sees a rise in the experimental heat transfer coefficient. The influence of the nucleate and bubble phenomena embodied in this mechanism appears to be significantly greater than any enhancement of the convective coefficient and we conclude there is no need to include any nucleate enhancement of h_{conv}, even in laminar flows.

Some enhancement of the single-phase heat transfer component is observed in some cases, especially in laminar flows. Since the effect is seen even when the walls are below the fluid saturation temperature, it is believed that this effect is due to inadequate outgassing of the test samples, leading to gas release and bubble formation as the fluid is heated through the subcooled region. The effect could be attributed to traces of dissolved gas (mass fraction <0.1%) and was generally insignificant once ONB occurred. The observation therefore does not impact significantly on the conclusions of this work but does confirm that even non-boiling two-phase flows may offer enhanced performance relative to their single-phase counterparts in microchannel heat transfer.

Acknowledgement

Financial support for this work has been provided by Heatric Ltd.

References

[1] J.G. Collier, J.R. Thome, Convective Boiling and Condensation, third ed., Oxford Science, Oxford, 1996.
[2] J.J. Schröder, Heat transfer in subcooled boiling, in: Chapter Hba in VDI Heat Atlas, VDI Verlag, Düsseldorf, 1993.
[3] S.G. Kandlikar, Heat transfer characteristics in partial boiling, fully developed boiling, and significant void flow regions of subcooled flow boiling, Journal of Heat Transfer 120 (1998) 395–401.
[4] A.E. Bergles, W.M. Rohsenow, The determination of forced-convection surface-boiling heat transfer, Journal of Heat Transfer 86 (1964) 365–372.
[5] J.C. Chen, Correlation for boiling heat transfer in to saturated fluids in convective flow, I and EC Process Design and Development 5 (1966) 322–329.
[6] D. Steiner, J. Taborek, Flow boiling heat transfer in vertical tubes correlated by an asymptotic model, Heat Transfer Engineering 13 (1992) 43–69.
[7] Z.-Y. Bao, D.F. Fletcher, B.S. Haynes, Flow boiling heat transfer of Freon R11 and HCFC123 in narrow passages, International Journal of Heat and Mass Transfer 43 (2000) 3347–3358.
[8] J.R. Baird, Z.-Y. Bao, D.F. Fletcher, B.S. Haynes, Local flow boiling heat transfer coefficients in narrow conduits, Multiphase Science and Technology 12 (2000) 129–144.
[9] Z.-Y. Bao, D.F. Fletcher, B.S. Haynes, An experimental study of gas–liquid flow in a narrow conduit, International Journal of Heat and Mass Transfer 43 (2000) 2313–2324.
[10] Z.-Y. Bao, Gas–liquid two-phase flow and heat transfer in fine passages, PhD Thesis, The University of Sydney, 1995.
[11] J.R. Baird, Phase-change heat transfer in narrow passages, PhD Thesis, The University of Sydney, 2001.
[12] M.O. McLinden, S.A. Klein, E.W. Lemmon, A.P. Peskin, Thermodynamic and Transport Properties of Refrigerants and Refrigerant Mixtures, NIST Standard Reference Database 23, Version 6.01, 1998.
[13] V. Gnielinski, New equations for heat and mass transfer in turbulent pipe and channel flow, International Chemical Engineering 16 (1976) 359–368.
[14] R.H. Notter, C.A. Schleicher, A solution to the turbulent Graetz problem. III. Fully developed and entry region heat transfer rates, Chemical Engineering Science 27 (1972) 2073–2093.
[15] R.K. Shah, A.L. London, Laminar Flow Forced Convection in Ducts: A Source Book for Compact Heat Exchanger Analytical Data, Academic Press, New York, 1978.
[16] D. Gorenflo, Pool boiling, in: Chapter Ha in VDI Heat Atlas, VDI Verlag, Düsseldorf, 1993.
[17] B. Palm, Heat transfer in microchannels, Microscale Thermophysical Engineering 5 (2001) 155–175.
[18] M.G. Cooper, Saturation nucleate pool boiling, a simple correlation, Institution of Chemical Engineers Symposium Series 86 (1984) 785–793.